Iraqi Journal of Physics, 2018 *Vol.16, No.38, PP. 99-111*

DOI: 10.20723/ijp.16.38.99-111

Improvement of superconducting parameters of $Bi_{1.6}Pb_{0.4}Sr_2Ca_2Cu_3O_{10+\delta}$ added with Au nanoparticles

Amal K. Jassim

Department of Physics, College of Science, University of Baghdad, Baghdad, Iraq

E-mail: amelmaliki@gmail.com

Abstract

Samples of $Bi_{1.6}Pb_{0.4}Sr_2Ca_2Cu_3O_{10+\delta}$ superconductor were prepared by solid-state reaction method to study the effects of gold nanoparticles addition to the superconducting system, Nano-Au was introduced by small weight percentages (0.25, 0.50, 0.75, 1.0, and 1.25 weight %). Phase identification and microstructural characterization of the samples were investigated using XRD and SEM. Moreover, DC electrical resistivity as a function of the temperature, critical current density *Jc*, AC magnetic susceptibility, and DC magnetization measurements were carried to evaluate the relative performance of samples. x-ray diffraction analysis showed that both (Bi,Pb)-2223 and Bi-2212 phases coexist in the samples having an orthorhombic crystal structure. Both the onset critical temperatures *Tc* (onset) and zero electrical resistivity critical temperatures *Tc* (*R*=0) of the samples were determined from the DC electrical resistivity measurements. An improvement of the superconducting transition temperature of 6.36 % was obtained with increasing Au nanoparticles to *x* = 1.25 wt.%, while the critical current density is improved by 220 %. AC magnetic susceptibility measurement showed that the diamagnetic fraction and intergranular coupling of the *x* = 1.25 wt.% sample are greater than those of the others. The variation of magnetization with temperature (*M-T* curve) of the samples was measured by cooling the sample in zero fields (ZFC) and an applied field of 10 Oe (FC). The results of AC magnetic susceptibility and DC magnetization measurements were in good agreement with DC electrical resistivity measurement.

Key words

Bi(Pb)-2223, Au nanoparticle, magnetic properties, critical current density.

Article info.

Received: Jan. 2018
Accepted: Jan. 2018
Published: Sep. 2018

تحسين معلمات التوصيل الفائق للنظام $Bi_{1.6}Pb_{0.4}Sr_2Ca_2Cu_3O_{10+\delta}$ بأضافة الدقائق النانوية Au

امل كاظم جاسم

قسم الفيزياء، كلية العلوم، جامعة بغداد، بغداد، العراق

الخلاصة

بطريقة تفاعل الحالة الصلبة لغرض دراسة تأثيرأضافة $Bi_{1.6}Pb_{0.4}Sr_2Ca_2Cu_3O_{10+\delta}$ حضرت النماذج فائقة التوصيل دقائق الذهب النانوية للنظام وبنسب وزنية صغيرة مساوية الى (0.25, 0.50 , 0.75, 1.0 ,1.25٪). وقد تم تشخيص الاطوار وتحديد الخصائص التركيبية للعينات باستخدام جهاز حيود الاشعة السينية والمجهر الالكتروني الماسح. أجريت قياسات المقاومية الكهربائية المستمرة كدالة لدرجة الحرارة وكثافة التيار الحرج والقابلية المغناطيسية والمغنطة المستمرة لتقييم الأداء النسبي للعينات.بينت تحليلات الاشعة السينية وجود الطورين Bi-2223, Bi-2212 وان التركيب البلوري معيني قائم. تم حساب كل من Tc (onset) و Tc

(R=0) من قياسات المقاومية الكهربائية المستمرة .ووجد تحسن في درجة الانتقال للتوصيل الفائق بمقدار 36. ٪ عند زيادة نسبة الذهب الى (*x* = 1.25 wt.%,) بينما كثافة التيار الحرج سوف تتحسن بمقدار% 220. قياسات القابلية المغناطيسية المتناوبة بينت ان الاقتران الحبيبي للنموذج x=1.25 اعلى من بقية النماذج. كما تم قياس تغييرالتمغنط مع درجات الحرارة (*M-T* curve) وذلك بتبريد العينة في مجال مساوي الى الصفر (ZFC) وكذلك في مجال مساوي الى (FC) 10 Oe. نتائج القابلية المغناطيسية المتناوبة وقياسات التمغنط كانت مطابقة لنتائج المقاومية الكهربائية المستمرة.

Introduction

Many studies concerning the preparation techniques, structural and superconducting properties of Bi-based superconductors have been carried out [1-4]. Doping is believed to be promising. It favors the 2223 phase formation and improves superconductivity. It is well established that the improvement of preparation process of high-T_C superconductor and its conducting properties is important for practical applications. Similarly, the effect of doping on the 2223 phase formation and its superconductivity is also influenced by the preparation condition. The BSCCO system mainly contains three phases in the general formula $Bi_2Sr_2Ca_{n-1}Cu_nO_{2n+4+y}$ (where n = 1, 2 and 3 refers to the number of CuO_2 layers which yields 10, 85, and 110 K transition temperatures, respectively), these three phases Bi-(2201), Bi-(2212), and Bi-(2223) are commonly have a multiphase structure [5]. Among the three phases of high-Tc bismuth superconductors, Bi-2223 is the most attractive materials that have been investigated extensively because it has the highest superconducting critical temperature.

It is difficult to align well the superconducting grains of the complex formation mechanism of the Bi-2223 phase. However, the grain connectivity and the degree of texturing in the samples depend on various parameters. It has been widely proved that the starting composition, several times of intermediate grinding, sintering time and temperature, have a strong influence on the Bi-2223 phase [6]. On the other hand, the formation and stability of this phase can be modified by the addition or substitution of elements of varying ionic radii and bonding characteristics. This variation is thought to be related to the density of charge carriers in the CuO planes [7]. The approval of a material for application in the Bi(Pb)SrCaCuO system necessitates the ability to control the effect of different doping elements and processing parameters on its properties.

The influence of dopant materials into the Bi-based superconductors has been found to improve formation and stability of the Bi-2223 phase [8, 9]. Pb is the most important doping element that influences the microstructure, phase composition and the related superconducting properties of the BSCCO system. The presence of Pb in the initial mixture, usually as PbO, favors the reaction kinetics of the 110 K phase. Pb addition results in the creation of a superconducting solid solution of $Bi_{2-x}Pb_xSr_2Ca_2Cu_3O_{10}$ by partial substitution of Bi [10-13]. Recently, the effect of nano addition has been extensively studied to improve the superconducting properties and to enhance the pinning force for BSCCO using nanoelements, nano-oxides, and nano-compounds [14-20]. The critical current density *Jc* is a crucial parameter of high-temperature superconductor for a variety of possible applications. The temperature dependencies of the critical current density may provide important information for identifying the flux pinning mechanism.

Superconductor critical current density in an applied magnetic field

was found to be increased when nanoparticles were added in the sample [21], which can be attributed to the presence of the flux pinning centers. By pinning the flux line effectively, vortex movement can be prevented. Hence, the critical current density is increased. A strong interaction between flux line network and magnetic texture can be expected if the magnetic impurities have the same order magnitude with the flux line network. By adding nanoparticles as pinning centers, the critical current density of superconductors can be enhanced [22-26].

In this work, the superconducting and transport properties of (Au)x $Bi_{1.6}Pb_{0.4}Sr_2Ca_2Cu_3O_{10}$ (x = 0, 0.25, 0.5, 0.75, 1.0, and 1.25 wt.%) specimens were investigated. The addition of Au nanoparticle is introduced as flux pinning centers to enhance the transport critical current density of BSCCO. Measurements of electrical resistivity (R-T), AC magnetic susceptibility, and DC magnetization (*M-T* curve) as a function of temperature and intergrain properties of Bi-2223 superconductors by using scanning electron microscopy (SEM) have been discussed. Also, x-ray diffraction analysis (XRD) has been reported in order to calculate the lattice parameter and the relative portion of both Bi-2223 and Bi-2212 phases.

Experimental work

Samples of nominal composition $Bi_{1.6}Pb_{0.4}Sr_2Ca_2Cu_3O_{10+\delta}$ were synthesized using a solid state reaction method. Au nanoparticles were added by small weight percentages (0.25, 0.50, 0.75, 1.0, and 1.25 wt%) in the first step of the synthesis process. High purity powders (99.99%) of Bi_2O_3, Pb_3O_4, $Sr(NO_3)_2$, CaO, CuO, and Au were mixed together by using a mill machine (SPEX Industries Inc.-USA), for a period of 15 minutes followed by manually grinding of powder using agate mortar and pestle for 15 minutes. The mixture homogenization takes place by adding a sufficient quantity of 2-propanol to form a paste during the process of grinding. The mixture was ground to a fine powder and then calcined in air by using a tube furnace at 810˚C for 24 h with a heating and cooling rate of 2˚C/min. The mixture was then pressed into pellets of diameter 13 mm and thickness (2-3) mm by using a hydraulic press (SPECAC) under a pressure of 0.7 GPa. The pellets were sintered at 845˚C for 140 hr. Pure BiPbSrCaCuO pellet (0 wt% Au) was prepared for comparison. XRD, EDX, and SEM were used for the structural investigations of the samples. DC electrical resistivity (R-T), critical current density *Jc*, AC magnetic susceptibility and DC magnetization measurements were conducted to study the superconducting properties of the prepared samples. The X-ray diffraction pattern for the samples was obtained using CuKα (1.54 Å) radiation in the range 2θ = 20–60˚ by Shimadzu-6000 Diffractometer. Volume fraction of the present phases was obtained from these patterns. A computer program was used to calculate the lattice parameters, based on Cohen's least square method. The surface morphology and grain structure of the samples were studied by scanning electron microscopy (SEM) (FEI Co. system SN: 9922650 – 2013/ Holland). The *R–T* curves of the samples were studied in order to determine the superconducting transition temperature (T_c). The electrical resistance measurements and the critical current density *Jc* for the samples were measured by using the four-probe technique. The magnetic properties measurements were carried out employing a Quantum Design

SQUID magnetometer MPMS-XL7 with an applied magnetic field of 10 Oe (FC) using the zero-field-cooled mode, that is, by cooling the sample at zero fields to 2 K, then applying a magnetic field and collecting data during the warming up process. The mutual inductance bridge method was used for the AC magnetic susceptibility measurements in 50–150 K temperature range.

Results and discussion

XRD patterns for $(Au)_xBi_{1.6}Pb_{0.4}Sr_2Ca_2Cu_3O_{10+\delta}$ where x = 0, 0.25, 0.5, 0.75, 1.0, and 1.25 wt.%, are shown in Fig. 1. The patterns indicate that all the samples have an orthorhombic structure and consisted of two phases; Bi-2212 and Bi-2223, with Bi-2223 being the dominant phase [27] in addition to a weak impurity phases of $Sr_2Ca_2Cu_7O$ at 2θ = 36.8˚, and Ca_2PbO_4 peak at 2θ = 32.5^o were identified in some samples. Similar results were obtained by Mawassi et al. [28] and Tanaka et al. [29]. No peaks belong to Au nanoparticles were found in the XRD pattern as the amount of addition is very low and it was incorporated into the crystal structure. This means that Au nanoparticle does not enter the crystal structure of the BSCCO system and does not lead to a variation in the crystal structure of the samples. To estimate the volume fraction of the present phases, the corresponding Bi-2212 and Bi-2223 peaks were used in the following formulas [30]:

$$V_{H(Bi-2223)} = \frac{\sum I(2223)}{\sum I(2223) + \sum I(2212)} \times 100\%$$

$$V_{L(Bi-2212)} = \frac{\sum I(2212)}{\sum I(2223) + \sum I(2212)} \times 100\%$$

where I (2223) and I (2212) are the intensities of Bi-2223 and Bi-2212 phases respectively. The volume fraction and the lattice parameters of the (Bi,Pb)-2223 superconducting samples added with Au are listed in Table 1. The relative volume fraction of (Bi,Pb)-2223 decreases with increasing the Au nanoparticles addition. Moreover, the transformation process of the (Bi,Pb)-2212 phase into (Bi,Pb)-2223 phase is impeded and retarded by the presence of nanoparticles [31,32]. The crystal structure of Au-free sample was found to be orthorhombic with the lattice parameters a=5.396432 Å, b=5.419031 Å and c = 37.11888Å. Almost, the same lattice parameters were obtained for the Au nanoparticles added samples. Increasing Au nanoparticles fraction to x=1.25 wt% slightly enhances the c-axis. There is no distortion in the crystal structure of the Au-added samples, which shows that Au nanoparticles do not participate in the crystal structure of the (Bi,Pb)-2223. This means that the added nanoparticles are sited between the superconducting grains. Furthermore, the role of such impurity nanoparticles can be either as the pinning centers to fix vortices or enhancing connectivity between grains, which may lead to higher Jc [33].

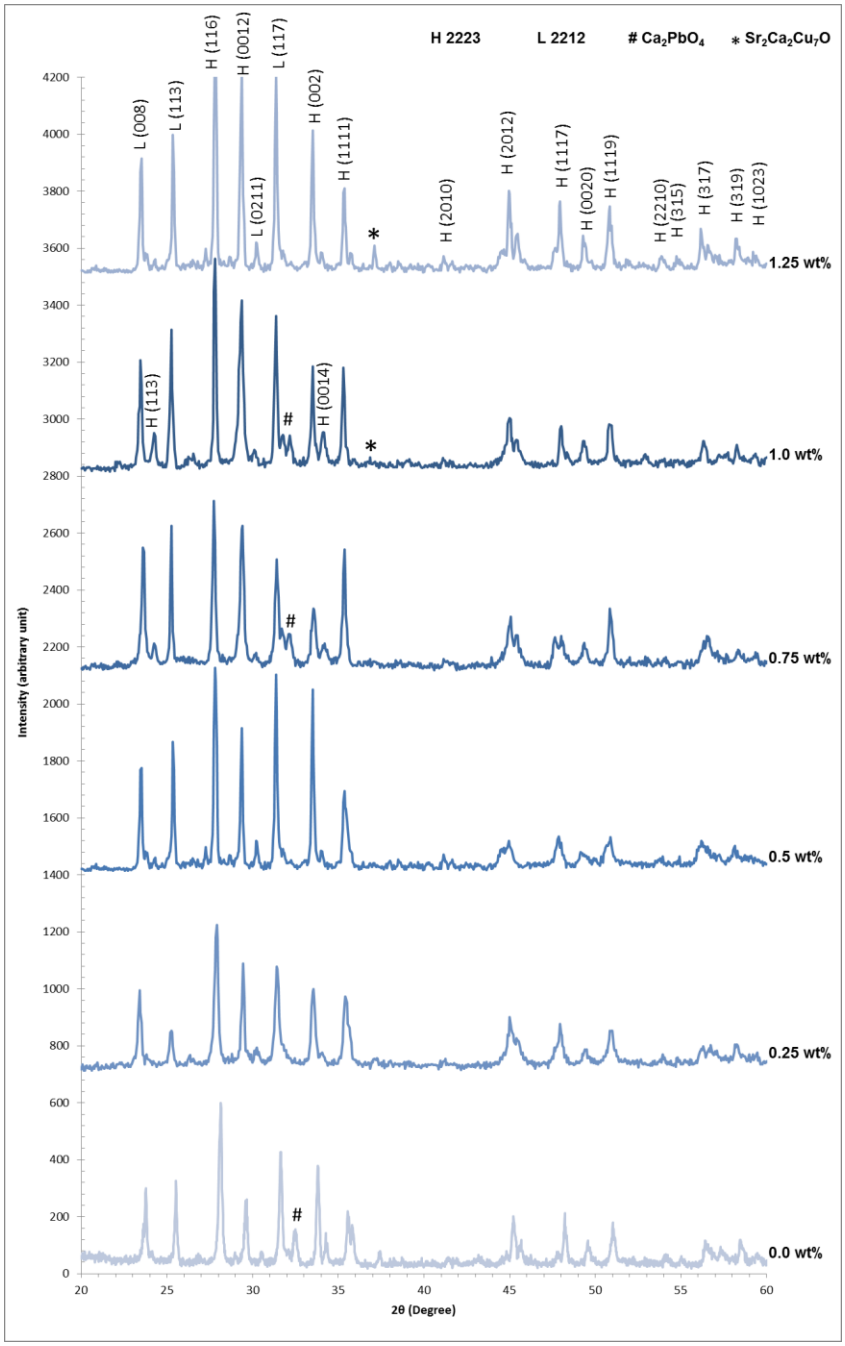

Fig.1: X-Ray diffraction patterns of $(Au)_xBi_{1.6}Pb_{0.4}Sr_2Ca_2Cu_3O_{10+\delta}$, where x = (0, 0.25, 0.5, 0.75, 1.0, and 1.25 wt%)

Table 1: Lattice parameters and phase volume fraction of $(Au)_xBi_{1.6}Pb_{0.4}Sr_2Ca_2Cu_3O_{10+\delta}$ samples for different Au nanoparticles weight percentage.

Nano-Au wt.%	a A°	b A°	c A°	$\frac{c}{a}$	Volume Fraction	
					HT_c%	LT_c %
0.0	5.396432	5.419031	37.11888	6.8784	69.07	30.93
0.25	5.393031	5.428991	37.11920	6.8828	72.14	27.86
0.50	5.391864	5.418775	37.11959	6.8501	75.54	24.46
0.75	5.394778	5.424538	37.12017	6.8807	78.16	21.84
1.0	5.392425	5.419431	37.12293	6.8499	80.02	19.98
1.25	5.396303	5.419551	37.12518	6.8503	80.25	19.75

The SEM micrographs of the surface view of the Au nanoparticles-free and -added samples are shown in Fig. 2. Superconducting grains are seen to be connected with each other strongly and the surface morphology of the samples comprises of a common feature of platelets and layered grains with uniform and homogenous microstructure. The grain size is larger in the Au nanoparticles added samples. As the weight % of Au nanoparticles increases, the size of platelets gradually increases. This means that increasing Au addition concentration to 1.25 wt% does not hinder the grains growth; on the contrary it increases the formation of randomly bigger platelet grains on the surface. Flower like grains were also observed, which may enhance the connectivity among the grains and they can increase the pinning centers to fix the vortices [34]. SEM results corroborate well with XRD results. In addition to the intergranular distribution of the nanoparticles, the presence of the nanoparticles can be observed in the other parts of microstructure of Au-added samples. Grains size of the 1.25 wt% sample increases comparing to the other samples, which may cause an increase in the superconducting properties of this sample.

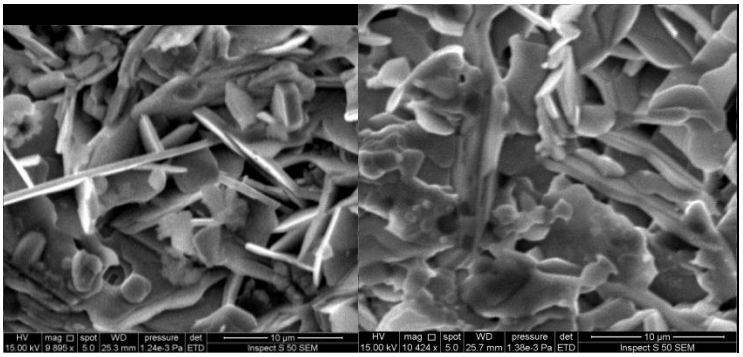

0.0 wt% Nano-Au 0.25 wt% Nano-Au

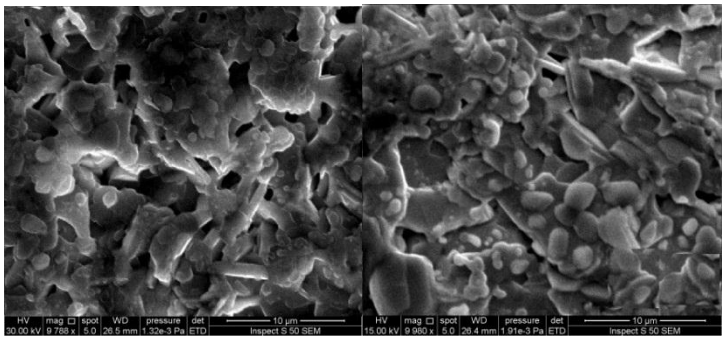

0.5 wt% Nano-Au 0.75 wt% Nano-Au

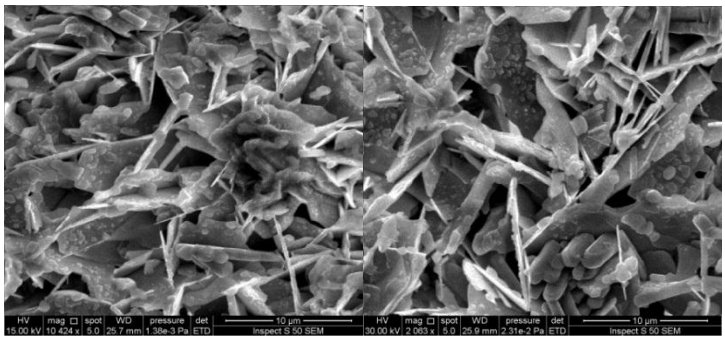

1.0 wt% Nano-Au 1.25 wt% Nano-Au

Fig. 2: SEM surface micrographs of $(Au)_xBi_{1.6}Pb_{0.4}Sr_2Ca_2Cu_3O_{10+\delta}$ samples, where x = 0.0 - 1.25wt.%

The variation of the DC electrical resistance with temperature (R-T) for (Au)$x$$Bi_{1.6}Pb_{0.4}Sr_2Ca_2Cu_3O_{10+\delta}$ with x = 0, 0.25, 0.5, 0.75, 1.0, and 1.25 wt.%, is shown in Fig. 3. All the samples displayed a metallic-like behavior at high temperature followed by a superconducting transition as the temperature is lowered. The plots show that the onset temperatures *Tc* (onset) of the sample 0.0wt% is in the close vicinity of 110 K. *Tc* (onset) for other samples are slightly increased to 108 K with increasing Au addition concentration to 1.25wt%. The zero resistivity critical temperature T_0 for Au free sample (x = 0.0 wt%) was 108 K and the transition temperature width (ΔTc) was narrower than those of the other samples. Since the *Tc* (onset) for sample 1.25 wt.% is the highest, the DC electrical resistance measurement show a good result for this sample, means that increasing Au nanoparticles addition to the BSCCO system resulted in increasing of both ΔTc and inter-grain connectivity [35], which consequently increase intergranular *Jc*. This result is in a good agreement with the XRD and SEM results where an increase in the grain size was observed and caused an enhancement in their superconducting properties. *Tc* for all samples is tabulated in Table 2. The variation of *Tc* with Au nanoparticles content *x* is shown in Fig. 4.

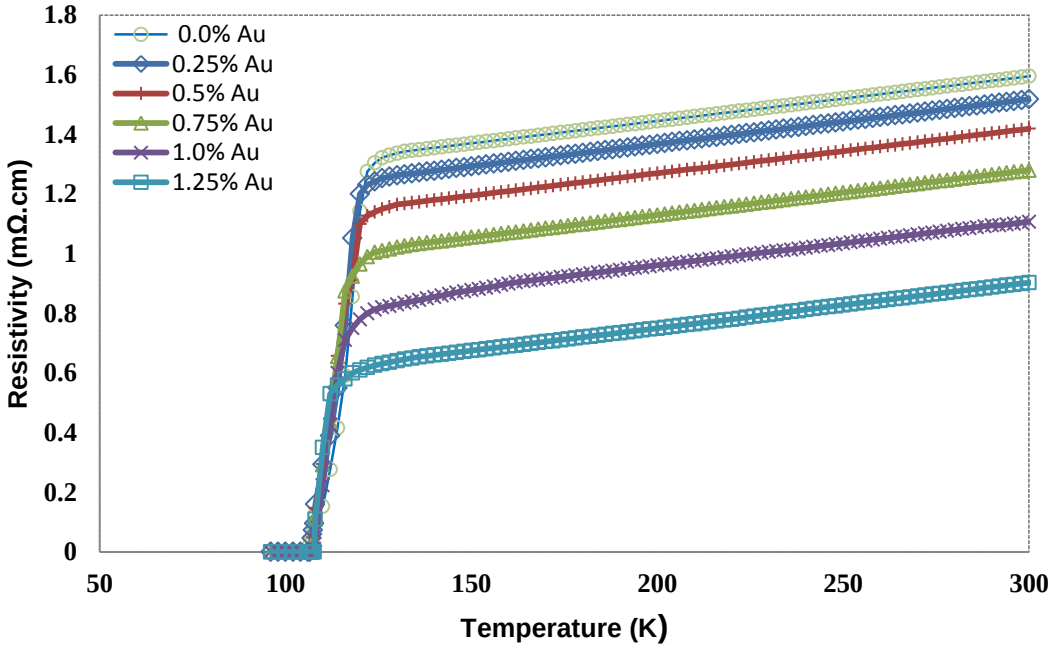

Fig. 3: ρ-T plots of (Au)$_x$$Bi_{1.6}Pb_{0.4}Sr_2Ca_2Cu_3O_{10+\delta}$ samples with x = 0.0 - 1.25 wt.%.

Table 2: The residual resistivity ρ_0, normal state resistivity ρ_n, T_c, $T_{c\,R=0}$, transition width ΔT_c and Jc of (Au)$_x$$Bi_{1.6}Pb_{0.4}Sr_2Ca_2Cu_3O_{10+\delta}$ samples with x = 0 - 1.25wt.%

(Au-NPs) wt%	ρ_0(mΩ.cm)	ρ_n(Mω.cm)	T_c (K)	T_0 (K)	ΔT_c (K)	Jc (A/cm^2)
0.0	0.1602	0.930	110	108	2	16.91
0.25	0.1545	0.875	110.7	107.7	3	20.35
0.50	0.1432	0.792	112	107.9	4.1	25.50
0.75	0.1277	0.720	113.5	108	5.5	30.08
1.0	0.1154	0.665	115.2	107.5	7.7	34.77
1.25	0.9112	0.627	117	108	9	37.28

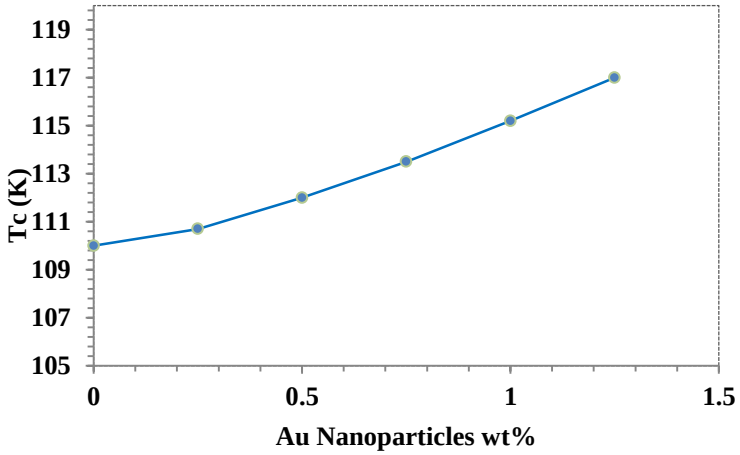

Fig. 4: Variation of critical temperature T_c and the Au nanoparticles weight percentage.

The critical current density for the samples of x = 0.0 – 1.25 wt% was measured at 77K in zero magnetic field as shown in graph of V – J curves in Fig. 5. *Jc* values of all samples are given in Table 2. It can be noticed that the results show an enhancement in the critical current density of the Au nanoparticles added samples as compared to the Au-free sample, this enhancement is proportional to the concentration of the Au in the samples. The critical current density improvement may be attributed to the enhancement in the flux pinning and the connectivity between the grains.

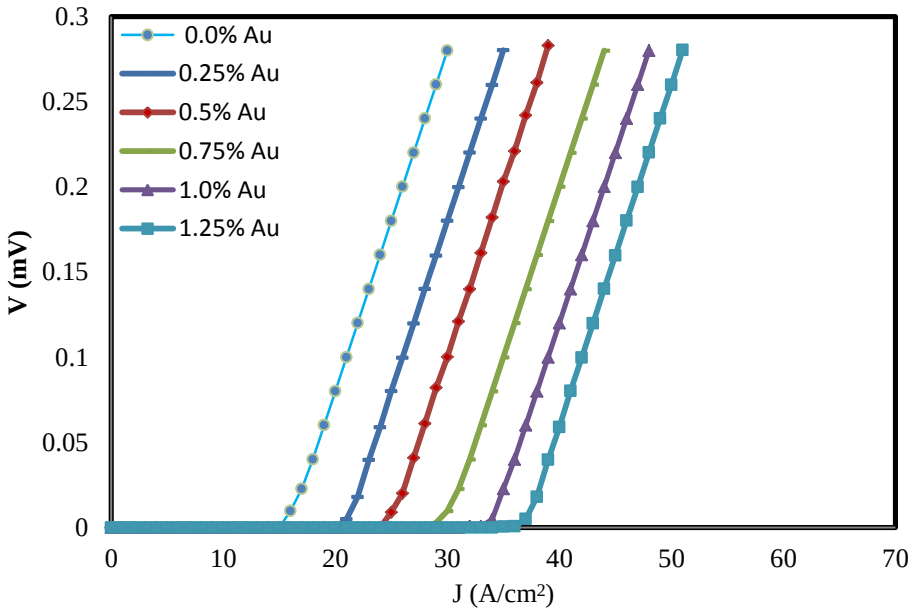

Fig. 5: Critical current density of $(Au)_xBi_{1.6}Pb_{0.4}Sr_2Ca_2Cu_3O_{10+\delta}$ samples with x = 0.0, 0.25, 0.5, 0.75, 1.0 and 1.25 wt.%.

The measurement of the real part χ' of the AC magnetic susceptibility on the $(Au)_xBi_{1.6}Pb_{0.4}Sr_2Ca_2Cu_3O_{10+\delta}$ samples is widely used as a nondestructive method for determination and characterization of the intra-and inter-grain features of the high temperature superconductors. This measurement was done for all the samples. The real parts of the AC susceptibility versus temperature measurements of samples are shown in Fig. 6. It is clearly showing that there are two phases. The figure displays

two significant drops as the temperature is decreased below *Tc* for granular superconductors which reflect the flux penetration between and into the grains, as temperature decreases. Therefore χ', is proportional to an amount of flux penetration into the body of the superconductor [39]. Correspondingly, the derivative of the χ' (T) displays two peaks. The first sharp drop for the Au-free sample in χ' seems to occur at *Tc* around 109 K is due to the transition within grains. Another drop in diamagnetic signal is observed around 105 ± 1 K is due to the occurrence of the superconducting coupling between grains, where superconducting current flows from grain to grain [40]. This second phase has comparatively slow transition and it reflects the presence of low-*Tc* (2212) component, which is also confirmed by X-ray analysis. Almost same behavior of susceptibility versus temperature curves was obtained for all the samples. However, the intergrain transition temperature shows an increase directly proportional to Au nanoparticle concentration starting from 110 K for Au-free sample and reaching 117 K for the 1.25 wt.% sample. These results suggest that Au nanoparticle-added samples up to *x*=1.25 wt.% have a better intergranular coupling between the grains, which is in good agreement with DC electrical resistivity measurement.

The realization of DC magnetization measurements (M-T curves) is based on ZFC (zero-field cooling) and FC (field-cooling) procedures in a superconducting sample. The DC magnetization (M) was measured for all samples in ZFC and FC states with an applied magnetic field of 10 Oe and a temperature range (2-150) K, as shown in Fig. 7. For the Au-free sample, it can be observed that when the sample is zero field cooled, it showed sharp diamagnetic transition at 110 K, as in the case of $\chi'(T)$. When the sample is field cooled, the applied external field is trapped, which implies existence of very strong pinning. ZFC and FC magnetization on Au added samples as a function of temperature was recorded. A sharp drop corresponding to the superconducting transition was observed in all the samples within a critical temperature range 110 – 116 K which is in good agreement with AC magnetic susceptibility and DC electrical resistivity measurements.

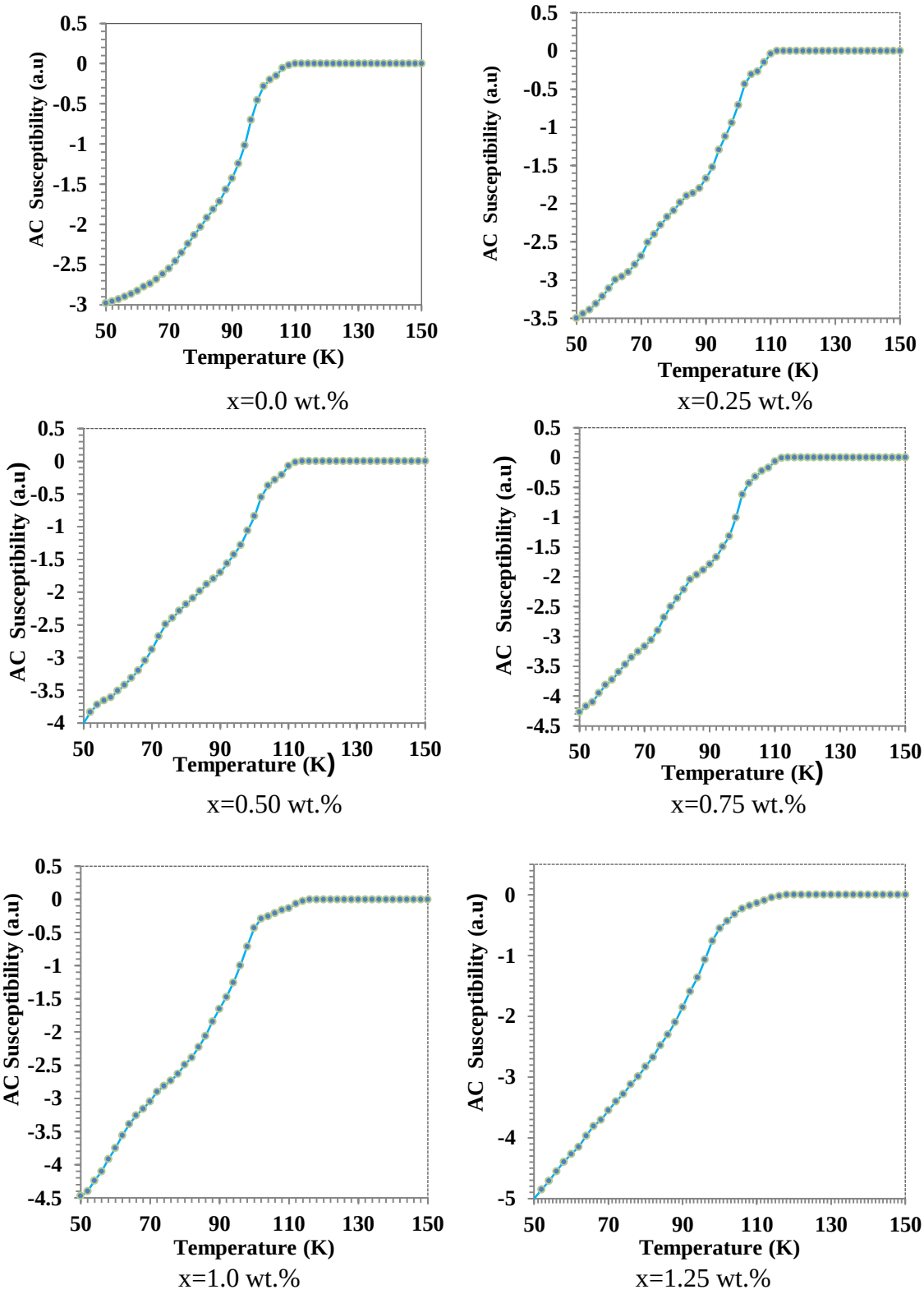

Fig. 6: Temperature dependence of the real part of AC susceptibility of $(Au)_xBi_{1.6}Pb_{0.4}Sr_2Ca_2Cu_3O_{10+\delta}$ samples with x = 0 - 1.25 wt.%.

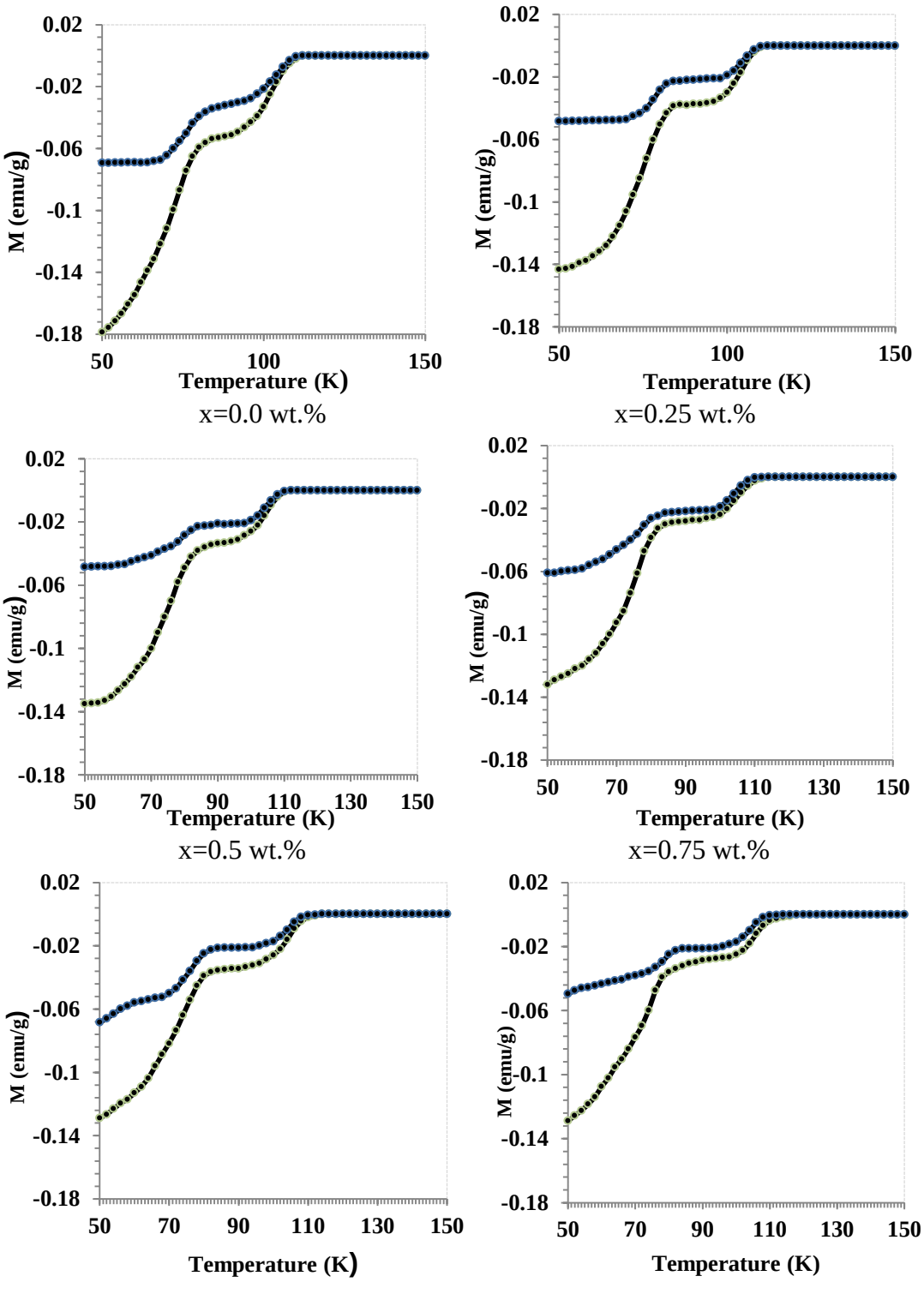

Fig. 7: M–T dependences of $(Au)_xBi_{1.6}Pb_{0.4}Sr_2Ca_2Cu_3O_{10+\delta}$ samples with x = 0 - 1.25 wt.%, measured in zero-field cooled (ZFC) and field cooled (FC).

Conclusions

The influence of Au nanoparticles addition on the phase formation and superconducting properties revealed that the high-*Tc* phase in the (Bi,Pb)-2223 system by means of gold addition in the form Au can be obtained. XRD analysis indicated that both Bi-2223 and Bi-2212 phases coexisted in the samples. The volume fraction of the

Bi-2223 decreased with increasing the Au-nano concentration. SEM results showed that the Au-nanoparticles settled among the grains boundaries without affecting the grain shape and improved the grain connectivity. The superconducting transition temperature enhanced with rate of 6.36 %, while, critical current density measurement showed an enhancement in the *Jc* values with rate of 220% with increasing Au nanoparticle concentration up to x = 1.25 wt%. This enhancement was attributed to the improvement of grain connectivity and flux-pinning. The AC magnetic susceptibility measurements for the samples show that the diamagnetic fraction and intergranular coupling of the sample of x = 1.25 wt.% are greater than those of the others which results in better superconducting properties of the samples. The ZFC and FC curves of the samples are found after final sintering at 845°C and show that the magnetic onset transition point is close to the DC resistive transition point.

References

[1] H. Maeda, Y. Tnaka, M. Fukutomi, T. Asano, Jpn. J. Appl. Phys., 27 (1988) L209-L210.

[2] H. Imao, S. Kishida, H. Tokutaka, Physica Status Solidi (a), 148 (1995) 537-543.

[3] H. Sozeri, N. Ghazanfari, H. Ozkan, A. Kilic, Super. Sci. Tech., 20, (2007) 522-528.

[4] C. Michel, M. Hervieu, M.Borel, A. Grandin, F. Deslandes, J. Provost, B. Raveau, Z. Phys. B. 68 (1987) 421-423.

[5] I. H. Gul, F. Amin, A. Z. Abbasi, M. Anis-ur-Rehman, A. Maqsood, Physica C. 449 (2006) 139-147.

[6] M. Nayera, A. Ramadan, A. Ali, I. Ibrahim, H. Mohamme, Materials Sciences and Applications, 3 (2012) 224-233.

[7] M. Tanako, J. Takada, K. Oda, H. Kitaguchi, Y. Miura, Y. Ikeda Y. Tomii, H. Mazaki, Japanese Journal of Applied Physics, 27 (1988) L1041-L1043.

[8] S. F.Oboudi, M. M. Abbas, N. Q. Raoof, International Journal of Engineering and Advanced Technology, 3 (2014) 94-97.

[9] G. Y. Hermiz, B. A. Aljurani, M. A. Al-Beayaty, Journal of Engineering and Advanced Technology, 3 (2014) 213-217.

[10] A. Jeremie, K. Alami-Yadri, J. Grivel, R. Flükiger, Superconductor Science and Technology, 6 (1993) 730-735.

[11] I. H. Gul, M. A. Rehman, M. Ali, A. Maqsood, Physica C 432 (2005) 71-80.

[12] O. Bilgili, Y. Selamet, K. Kocabas, J. Supercond. Nov. Magn. 21 (2008) 439-449.

[13] I.H. Gul, M.A. Rehman, A. Maqsood, Physica, C 450 (2006) 83-87.

[14] W. Kong, R. Abd-Shukor, Journal of Electronic Materials, 36 (2007) 1648-1651.

[15] M. A. Suazlinaa, S. Y. S. Yusainee, H. Azhan, R. Abd-Shukor, R. M. Mustaqim, Journal Teknologi (Sciences & Engineering) 69 (2014) 49-52.

[16] Z. Y. Jia, H. Tang, Z. Q. Yang, Y. T. Xing, Y. Z. Wamg, G. W. Qiao, 2000. Physica, C 337 (2000) 130-132.

[17] A. Ishii, T.Hatano, Physica, C 340 (2000) 173-177.

[18] W. Wei, J. Schwartz, K. C. Goretta, U. Balachandran, A. Bhargava, Physica, C 298 (1998) 279-288.

[19] S. E. M. Ghahfarokhi, N. Hoseenzadeh, M. Z. Shoushtari, J. Supercond. Nov. Magn. 27 (2014) 2217-2223.

[20] A. Biju, P. M. Sarun, R. P. Aloysius, U. Syamaprasad, Supercond. Sci. Technol., 19 (2006) 1023-1029.

[21] S. Y. Yahya, M. H. Jumali, C. H. Lee, R. Abd-Shukor, Journal of Material Science, 39 (2004) 7125-7128.
[22] I. F. Lyuksyutov, D. G. Naugle, Mod. Phys. Lett. B., 13B (1999) 491-508.
[23] B. A. Glowacki, M. Majoros, A. M. Campbell, S. C. Hopkins, N. A. Rutter, G. Kozlowski, T. L. Peterson, Supercond. Sci. Technol., 22, 034013 (2009) 1-10.
[24] K. T. Lau, S. Y. Yahya, Abd- R. Shukor, J. Appl. Phys., 99, 123904 (2006) 1-4.
[25] H. Baqiah, S. A. Halim, M. I. Adam, S. K. Chen, S. S. H. Ravandi, M. A. M. Faisal, M. M. Kamarulzaman, M. Hanif, Solid State Science and Technology, 17 (2009) 81-88.
[26] R. Abd-Shukor, W. Kong, J. Appl. Phys., 105, 07E311-2 (2009).
[27] J. M. Repaci, C. Kwon, X. G. Jiang, Q. Li, R. E. Glover, C. Lobb, J. Bull. Am. Phys. Soc., 40, 445 (1995).
[28] R. Mawassi, S. Marhaba, M. Roumié, R. Awad, M. Kork, I. Hassan, J. Super. Nov. Magn. 27 (2014) 1131-1142.
[29] Y. Tanaka, M. Fukutomi, T. Asano, H. Maeda, Japanese Journal of Applied Physics, 27 (1988) L548-L549.
[30] M. Zargar Shoushtari, S. E. Mousavi Ghahfarokhi, J. Super. Nov. Magn, 24 (2011) 1505-1511.
[31] E. Guilmeau, B. Andrzejewski, J.G. Noudem, Physica, C 387 (2003) 382-390.
[32] A. Ghattas, M. Zouaoui, M. Annabi, A. Madani, F. Ben Azzouz, M. Ben Salem, J. Phys. Conf. Ser., 97, 012179 (2008) 1-5.
[33] S. A. Halim, S. A. Khawaldeh, S. B. Mohamed, H. Azhan, Mater. Chem. Phys., 61 (1999) 251-259.
[34] K. Kocabas, M. Gökçe, M. Çiftçioglu, O. Bilgili, J. Super. Nov. Magn. 23 (2010) 397-410.
[35] K. Kocabas, M. Ciftcioglu, Phys. Stat Sol., (a) 177, 2 (2000) 539-545.
[36] O. Bilgili, Y. Selamet, K. Kocabas, J. Supercond Nov. Magn. 21, 8 (2008) 439-449.
[37] C. N. R. Rao J. Gopalakrishnan, A. K. Santra, V. Manivannan, Physica C Superconductivity, 174 (1991) 11-13.
[38] A. Zelati, A. Amirabadizadeh, A. Kompany, H. Salamati, J. Sonier, J. Super. Nov. Magn., 27 (2014) 1369-1379.
[39] N. Ghazanfaria, A. Kilic, A. Gencerb, H. Ozkana, Solid State Com., 144 (2007) 210-214.
[40] P. Kamali, H. Salamati, I. Abdolhosseini, Alloys Comp. J., 458, 1-2 (2008) 61-65.